Instabilities of Higher-Order Parametric Solitons. Filamentation versus Coalescence.

Dmitry V. Skryabin *, and William J. Firth
Department of Physics and Applied Physics, John Anderson Building,
University of Strathclyde, 107 Rottenrow, Glasgow, G4 0NG, Scotland, UK
URL: http://cnqo.phys.strath.ac.uk/∼dmitry
(December 23, 1997)

We investigate stability and dynamics of higher-order solitary waves in quadratic media, which have a central peak and one or more surrounding rings. We show existence of two qualitatively different behaviours. For positive phase mismatch the rings break up into filaments which move radially to initial ring. For sufficient negative mismatches rings are found to coalesce with central peak, forming a single oscillating filament.

Stability of optical solitary waves ('solitons') is one of the most important questions of theoretical nonlinear optics because of its direct connection with the possibility of experimental observation of solitons. Stability of the solitons in fully integrable systems naturally follows from integrability. Solitons of the one-dimensional (1D) Nonlinear Schröedinger Equation (NLS), describing propagation of short pulses in a fibre with cubic nonlinearity, are a well known example [1]. A wide range of the non-integrable hamiltonian models also have solitary solutions. For instance, equations describing parametric interaction in quadratic nonlinear media have solitary solution, which were pioneered in Refs. [2] and recently explored in details from both theoretical and experimental sides because of their many interesting features, see e.g. [3,4]. In non-integrable systems the stability of ground-state solitary solutions is often governed by the derivative of some integral invariant with respect to an associated free parameter of the solution [4–6]. For example, it has been rigorously proved that for ground-state bright solitary solutions of the generalized NLS equation positivity of the derivative of total energy with respect to the nonlinear wave number shift is a necessary and sufficient condition for stability [5]. Numerical and analytic studies indicate that this holds also for ground states in quadratic media [4].

Existence of higher-order solitary waves with bright and dark central spots surrounded by one or more rings was demonstrated for 2D NLS equation with pure Kerr [7] and saturable [5,8–10] nonlinearities and also in quadratic nonlinear media [10–12]. No universal stability criterion is known for higher-order bound states and their stability has to be studied individually in every case. It has been shown that for saturable nonlinearity higher-order bound states with bright and dark central spots are stable with respect to purely radial perturbations, obeying to criteria for ground states, but unstable with respect to azimuthally dependent perturbations, showing breakup of their rings into filaments [8–10]. Properties of solutions with dark central spot are strongly affected by their nonzero angular momentum and these properties are very similar for both saturable and quadratic nonlinearities [10].

Dynamics induced by instability of higher-order states is fascinating phenomena on its own and it is a natural starting point for understanding pattern forming phenomena in the evolution of higher-order gaussian beams in nonlinear media [13]. Primary interest of this Communication is to address (for the first time to our knowledge) problem of stability and dynamics of higher order solutions with zero angular momentum in quadratic media. In particular we show that these solutions reveal new scenario of evolution which is absent for corresponding solutions in Kerr-like media. Namely for some parameters values symmetry-breaking instability leading to filamentation along rings replaces with novel symmetry-preserving instability resulting in coalescence of rings with a central peak.

We consider interaction of first and second harmonic optical fields propagating in a dielectric medium with quadratic nonlinearity, under the conditions of type I phase matching and with negligible walk-off effects. The corresponding hamiltonian [2] is $H = \int\int dxdy\ [\frac{1}{2}|\vec{\nabla}_\perp E_1|^2 + \frac{1}{4}|\vec{\nabla}_\perp E_2|^2 + \beta|E_2|^2 - \frac{1}{2}(E_1^2 E_2^* + c.c.)]$, where $\vec{\nabla}_\perp = \vec{i}\partial_x + \vec{j}\partial_y$ and β is the normalized phase mismatch. All variables and parameters are dimensionless, and these scaled units are used throughout the text and in the figures. The evolution of the normalised field envelopes of the fundamental (E_1) and second (E_2) harmonics obeys the system of equations:

$$i\partial_z E_m = \frac{\delta H}{\delta E_m^*}, \quad m = 1, 2. \tag{1}$$

We look for non-diffracting solutions of Eqs. (1) in the form $E_m(z, x, y) = A_m(r)e^{im\kappa z}$, where $r = \sqrt{x^2 + y^2}$, A_m are real functions and κ is the nonlinear wave vector shift. The existence condition of localised solutions with exponentially decaying tails is $\kappa > max(0, -\beta/2)$. For any value of κ in this range we were able to numerically build higher-order many-ring solitary solutions with a bright central spot. Examples of spatial profiles of one- and two-ring solutions are presented in Fig. 1(a). For any finite number of rings, the fundamental field has radial zeroes but the second harmonic field always remains

positive, though having minima close to the zeros of the fundamental. In the limit $\beta \gg 1$ Eqs. (1) can be approximately reduced to an NLS equation for the fundamental field. Accordingly for increasing β the second harmonic field tends to carry less and less of the energy. The situation is opposite for negative β, when κ values are close to the boundary of soliton existence. Dependences vs κ of the energy invariant $Q = \int\int dxdy\ (|E_1|^2 + 2|E_2|^2)$ are presented in Fig. 1(b).

To study stability we consider 2D perturbations of these solutions in the general form $E_m(r,\theta,z) = e^{im\kappa z}(A_m(r) + \epsilon_m^+(r)e^{\lambda z + iJ\theta} + \epsilon_m^{-*}(r)e^{\lambda^* z - iJ\theta})$. Here θ is the polar angle and J is the azimuthal index of the perturbation. J must be an integer for azimuthal periodicity. Linearising Eqs. (1) and putting $\epsilon_m^{\pm} = r^{|J|} f_{Jm}^{\pm}(r)$ gives the non-self-adjoint eigenvalue problem:

$$i\lambda_J \begin{bmatrix} f_{J1}^+ \\ f_{J1}^- \\ f_{J2}^+ \\ f_{J2}^- \end{bmatrix} = \begin{bmatrix} \hat{L}_{J1} & A_2 & A_1 & 0 \\ -A_2 & -\hat{L}_{J1} & 0 & -A_1 \\ A_1 & 0 & \hat{L}_{J2} & 0 \\ 0 & -A_1 & 0 & -\hat{L}_{J2} \end{bmatrix} \begin{bmatrix} f_{J1}^+ \\ f_{J1}^- \\ f_{J2}^+ \\ f_{J2}^- \end{bmatrix}, \quad (2)$$

where $\hat{L}_{J1} = \frac{1}{2}\hat{R}_J - \kappa$, $\hat{L}_{J2} = \frac{1}{4}\hat{R}_J - 2\kappa - \beta$ and $\hat{R}_J = \frac{d^2}{dr^2} + \frac{2|J|+1}{r}\frac{d}{dr}$. We seek unstable eigenmodes in the class of functions obeying $\frac{df_{Jm}^{\pm}}{dr} = 0$ at $r = 0$ and exponentially decaying at $r \to \infty$. Corresponding eigenvalues belonging to the discrete spectrum can lie anywhere in the complex plane outside the rays $(i\Omega_c, i\infty)$ and $(-i\Omega_c, -i\infty)$ which belong to the stable unbounded continuum, here $\Omega_c = min(\kappa, 2\kappa + \beta)$. Unstable modes have eigenvalues with $Re\lambda_J > 0$. They must always have a counterpart with $Re\lambda_J < 0$ because of the hamiltonian nature of our problem. Infinitesimal phase and translational transformations of the stationary solutions generate two eigenfunctions: $\tilde{f}_{0m}^{\pm} = \pm m A_m$ for $J = 0$ and $\tilde{f}_{1m}^{\pm} = \frac{1}{r}\frac{dA_m}{dr}$ for $J = 1$, which are neutrally stable ($\lambda_{0,1} = 0$).

We will mainly deal with solutions with only one ring outside the central peak. These show the main features of the dynamics of solutions with an arbitrary number of rings. First we consider symmetry-preserving perturbations, $J = 0$. Using asymptotic techniques developed for the ground-state solution [4], it can be shown that the neutrally stable mode branches at the point $\partial_\kappa Q = 0$ giving instability for $\partial_\kappa Q < 0$, see Fig. 1(b). Thus we can conclude that the standard stability criterion for ground states [4,5] is also a *necessary* condition for stability of higher-order bound-states. This instability is related to the existence for $\partial_\kappa Q > 0$ of a pair of eigenmodes with purely imaginary eigenvalues (with opposite signs) lying in the gap $(-i\Omega_c, i\Omega_c)$. At the point $\partial_\kappa Q = 0$ these eigenmodes coincide with the neutral mode and for more negative β appear again but with purely real eigenvalues of opposite sign, signifying instability. For the ground-state this is the only instability scenario and these discrete eigenmodes disappear into the continuum for large $\beta > 0$ [14].

In the present system, we have undertaken numerical investigation of eigenvalue problem (2). The case $J = 0$ reveals two pairs of discrete eigenmodes. Interplay between them leads to a new bifurcation scenario, which we study for different values of β for fixed $\kappa = 3$. Changing κ at fixed β has no qualitative effect due to scaling properties of (1). However introducing this scaling modifies the stability criterion $\partial_\kappa Q > 0$ [4], which we prefer to avoid.

Real and imaginary parts of key eigenvalues from the discrete spectrum are plotted vs β in Fig. 2. In the limit of large β we found one internal eigenmode (line 1 in Fig. 2) but at $\beta \simeq 4.75$ another internal eigenmode (line 2) emerges from the continuum. On emergence mode 2 has $Im\lambda_0 = \kappa = 3$, but as β is decreased the eigenvalues of the two modes bring together, as Fig. 2 shows. They fuse at $\beta \simeq -0.82$ to form two pairs of eigenfunctions with complex conjugate eigenvalues, giving onset of an instability (lines 3,4). At $\beta \simeq -2.06$ a reverse bifurcation takes place (lines 5,6). One eigenmode (Fig. 3(a)) then has a purely imaginary eigenvalue (line 6) until it loses its stability at $\beta \simeq -5.61$ (line 7) where $\partial_\kappa Q = 0$. This is the standard instability scenario described above. The other eigenmode undergoes a similar bifurcation, but at $\beta \simeq -2.17$ (lines 5,8) which is well before the point $\partial_\kappa Q = 0$. At this bifurcation the eigenfunction profiles, Fig. 3(b), are quite different from those of the neutrally stable eigenmode. Thus, unlike the previously-known case (lines 6,7 and Fig. 3a) this new instability cannot be captured by asymptotic expansion around that neutral eigenmode. In both cases the unstable eigenvalues reach a maximum then go steeply to zero near the existence limit of solitary solutions, $\beta = -2\kappa$.

The cascade of symmetry preserving bifurcations presented in Fig. 2 is somewhat similar to that for TE_1 mode instability in a planar waveguide (1D geometry) with Kerr nonlinearity [15] where joint action of the refraction index discontinuties and field nodes leads to instability. In our situation the new symmetry-preserving instability develops in the region where the nodeless second harmonic starts to dominate over the fundamental, which has one or more nodes.

For symmetry-breaking perturbations, $J \neq 0$, the stability properties are not so rich as for $J = 0$. For $J = 1$ our numerics reveals the presence of a neutral mode and a pair of eigenmodes in the discrete spectrum with purely real eigenvalues, one of which is responsible for instability. We did not find any exchange of stability of these modes. For every J from 2 to 5 we find such a pair of discrete eigenmodes with purely real eigenvalues and all modes for $J > 5$ belong to the continuum. The unstable perturbations for $J = 3, 4$ are localised around the ring of the bound-state in a manner similar to what happens in saturable media [8].

To show how the character of instability of the one-ring solution depends on phase mismatch parameter we plot in Fig. 4 growth rates vs β for all unstable eigenmodes. For phase mismatches from the cascading limit

down to $\beta \sim -3$ symmetry breaking instabilities with $J = 3, 4$ are dominant. However, sufficiently far from the NLS limit our new scenario, with azimuthally homogeneous perturbations dominant, is realised. We stress again (see discussion above) that this symmetry preserving instability is not related to violation of the criterion $\partial_\kappa Q > 0$. Note that in the limit $\beta \gg 1$ the $J = 0$ internal eigenmode exists and the $J = 1$ eigenmode has non-zero growth rate (Fig. 4(b)).

One expects the propagation dynamics of solitary states to be mainly determined by the perturbation eigenmode with maximal growth rate. To examine this we performed an extensive series of numerical simulations of Eqs. (1), using both polar and cartesian grids. Predictions based on our stability analysis are in good agreement with the results of our simulations. An example of noise-stimulated break-up of a one-ring solution into three filaments is shown in Fig. 5(a). We plot the real part of the fundamental field profile rather than the intensity distributions to show that the daughter solitons formed from the ring are out of phase with the central one. Radiation losses in the break-up are quite small, so that the initial energy Q is mostly divided among the daughter solitons. Their diameters are comparable to the width of the initial ring. For β values where growth rates for $J = 3$ and $J = 4$ are almost equal the simulation results depended on the particular noise realisation, but we mostly observed the ring forming four filaments, one of which was usually less intense than the others.

Throughout the whole range of parameters where the symmetry-breaking instability is dominant we observed repulsion between the central spot and daughter filaments, which results from the fact they are out of phase [16], see Fig. 5(a). This repulsive force makes the outer filaments move out along radii (Fig. 5(b)), in contrast to the tangential motion of daughter solitons after breakup of one-ring solitary waves carrying non-zero orbital angular momentum [10], where inter-soliton forces are negligible in comparison to the need to conserve angular momentum.

Our stability analysis predicts a novel symmetry-preserving instability scenario where the $J = 0$ eigenmode dominates. This prediction is indeed confirmed by the simulations. For example, at $\beta = -4.2$, instead of fragmentation we observed coalescence of the ring with the central spot to form a single filament. After transient dynamics this filament forms an oscillating solitary wave, see Fig.6. These undamped pulsations are related to the existence of an internal eigenmode of the ground-state solution [14].

Considering now two-ring solitary solutions, we present the growth rates for the dominant eigenmodes and an example of symmetry- breaking instability, see Fig.7. General features of the dynamics are qualitatively similar to the one-ring situation.

The evolution of filaments following a symmetry breaking instability of peak-and-ring solitary solutions in saturable Kerr media [8] is a question which has not previously been examined. In simulations of this problem we observed the same sort of dynamics as described above for quadratic media, but with no coalescence phenomena.

In summary, we have undertaken a detailed analysis of stability of cylindrically-symmetric higher-order solitary waves due to parametric interaction in quadratic nonlinear media. For a wide range of positive mismatches, symmetry-breaking instability of the rings is predicted, and confirmed by simulations which show that the instability leads to filamentation into daughter solitons which are repelled radially from the central spot. For sufficiently negative phase mismatches we predict that a new symmetry- preserving instability becomes dominant. This is confirmed in simulations, in which the rings are found to coalesce with the central filament, forming an oscillating, single-peaked, solitary wave. To our knowledge this is the first explicit example of a symmetry-preserving instability of 2D self-trapped beams in bulk media different from the Vakhitov-Kolokolov scenario [5].

We thank G. K. Harkness, Y. Kivshar and A. Buryak for discussions of relevant questions and L. Torner for sharing with us Ref. [12] prior to publication. This work was partially supported by EPSRC grant GR/L 27916.

[1] V.E. Zakharov and A.B. Shabat, Sov. Phys. JETP, **34**, 62 (1972).

[2] Y.N. Karamzin and A.P. Sukhorukov, JETP Lett. **20**, 339 (1974); Sov. Phys. JETP **41**, 414 (1976).

[3] G.I. Stegeman, D.J. Hagan, and L. Torner, Opt. Quantum Electron. **28**, 1691 (1996) and refs. therein.

[4] D.E. Pelinovsky, A.V. Buryak, and Y.S. Kivshar, Phys. Rev. Lett. **75**, 591 (1995).

[5] M.G. Vakhitov and A.A. Kolokolov, Sov. Radiophys. **16**, 783 (1973).

[6] F.V. Kusmartsev, Phys. Rep. **183**, 1 (1989); R.L. Pego and M.I. Weinstein, Phil. Trans. R. Soc. Lond. A **340**, 47 (1992).

[7] H.A. Haus, Appl. Phys. Lett. **8**, 128 (1966); Z.K. Yankauskas, Sov. Radiophys. **9**, 261 (1966).

[8] J.M. Soto-Crespo, D.R. Heatley, E.M. Wright, and N.N. Akhmediev, Phys. Rev. A **44**, 636 (1991).

[9] V.I. Kruglov, Y.A. Logvin, and V.M. Volkov, J. Mod. Opt. **39**, 2277 (1992); J. Atai, Y. Chen, and J.M. Soto-Crespo, Phys. Rev. A **49**, R3170 (1994).

[10] W.J. Firth and D.V. Skryabin, Phys. Rev. Lett. **79**, 2450 (1997).

[11] H. He, M.J. Werner, and P.D. Drummond, Phys. Rev. E **54**, 896 (1996).

[12] J.P. Torres, J.M. Soto-Crespo, L. Torner, and D.V. Petrov, J. Opt. Soc. Am. B **15**, 625 (1998).

[13] V. Tikhonenko, J. Christou, and B. Luther-Davies, J. Opt. Soc. Am. B **12**, 2046 (1995); J. Courtial, K. Dholakia, L. Allen, and M.J. Padgett, Phys. Rev. A **56**, 4193 (1997); J.P. Torner and D.V. Petrov, J. Opt. Soc. Am.

B **14**, 2017 (1997); P. Agin and G.I. Stegeman, J. Opt. Soc. Am. B **14**, 3162 (1997).
[14] C. Etrich, U. Peshel, F. Lederer, B.A. Malomed, and Y.A. Kivshar, Phys. Rev. E **54**, 4321 (1996).
[15] H.T. Tran, J.D. Mitchell, N.N. Akhmediev, and A. Ankiewich, Opt. Commun. **93**, 227 (1992).
[16] Y. Baek, R. Schiek, G.I. Stegeman, I. Baumann, and W. Sohler, Opt. Lett. **22**, 1550 (1997); V. Steblina, A. Buryak, and Y.S. Kivshar, Opt. Lett. **23**, 156 (1998).

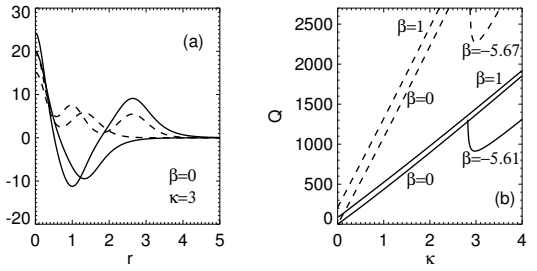

FIG. 1. (a) Radial profiles of one- and two-ring solitary waves. Full (dashed) lines are for A_1 (A_2). (b) Total energy vs κ for one-ring (full lines) and two- ring (dashed lines) solitary waves. The negative values of β are chosen so as to give $\partial_\kappa Q = 0$ at $\kappa = 3$.

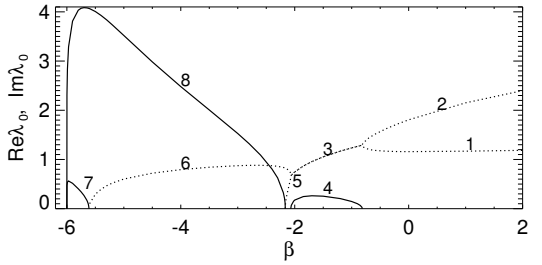

FIG. 2. Real (full lines) and imaginary (dotted lines) parts of the eigenvalues of $J = 0$ eigenmodes vs β, $\kappa = 3$.

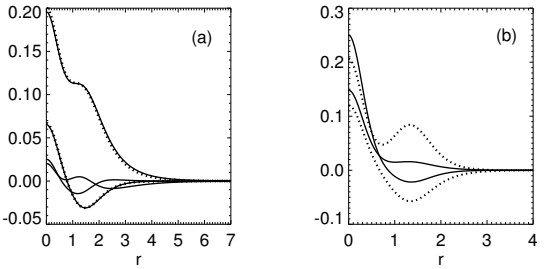

FIG. 3. (a) The internal eigenfunction corresponding to branch 6 in Fig. 2 at the point $\beta = -5.58$, slightly before the bifurcation point $\partial_\kappa Q = 0$. (b) The internal eigenfunction corresponding to the bifurcation point at $\beta = -2.17$ where branches 5,8 in Fig. 2 meet. Dots mark the neutrally stable eigenmode. $\kappa = 3$.

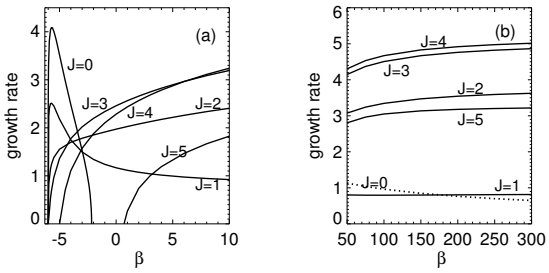

FIG. 4. Growth rates of the maximally unstable eigenmodes vs β for one-ring solitary solutions. Dotted line in (b) displays $Im\lambda_0$ of the $J = 0$ internal eigenmode marked by Line 1 in Fig. 2. $\kappa = 3$.

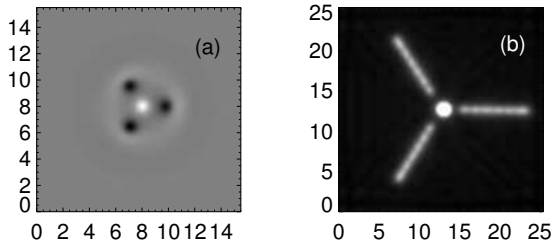

FIG. 5. (a) Real part of the fundamental harmonic field at a late stage of a simulation of the symmetry-breaking process. (b) Superimposed images of its transverse intensity distribution at different values of z, showing radial trajectories of the daughter solitons. $\beta = -1$, $\kappa = 3$. Brightness and size of central spot in Fig. (b) are exaggerated by the superposition of multiple images.

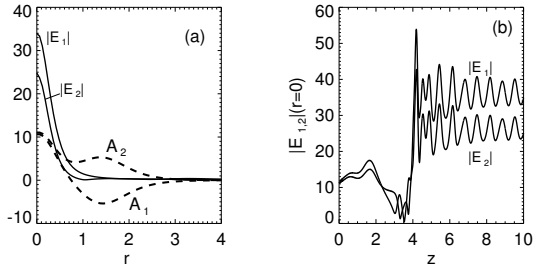

FIG. 6. (a) Initial (dashed lines) and post-coalescence (solid lines) radial profiles of fundamental and second harmonics simulated where the symmetry-preserving instability is predicted to dominate. (b) Corresponding evolution of $|E_{1,2}|$ at $r = 0$ vs propagation coordinate z. $\kappa = 3$, $\beta = -4.2$

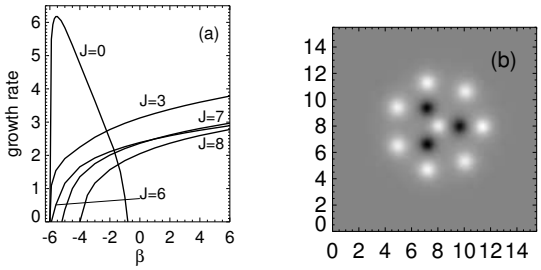

FIG. 7. (a) Growth rates of the dominant unstable eigenmodes vs β for two-ring solitary solutions. (b) Real part of the fundamental field at a late stage of a simulation of the symmetry-breaking process. $\beta = 1$, $\kappa = 3$.